In Situ Rheo-NMR Investigations of Shear-Dependent ^{1}H Spin Relaxation in Polymer Solutions

M. V. Badiger, P. R. Rajamohanan, P. M. Suryavanshi, S. Ganapathy, and R. A. Mashelkar*

National Chemical Laboratory, Pune 411 008, India

Received May 30, 2001

ABSTRACT: The NMR response of a polymeric fluid to the application of shear field has been studied by using specially designed shearing devices conforming to a couette geometry. We show that an air-driven high-resolution liquids sample spinning arrangement, available on any high-resolution liquid-state NMR spectrometer, is easily adapted to set up a couette cell and impart shear rates ($\dot{\gamma}$) of ca. 18−450 s^{-1} on polymer solutions of low viscosity. This simple but elegant method has allowed us to conduct in situ rheo-NMR relaxation experiments on poly(acrylamide) solution where we observe large changes in proton spin−lattice relaxation times in the sheared state of the polymer. The enhanced relaxation rates are rationalized on the basis of the release of entanglements due to breaking of intermolecular hydrogen bonds, which decrease the rotational correlation times for the molecular motions. By identifying from the 2-D NOESY experiments that the molecular mobility occurs in the long correlation regime ($\omega_0\tau_c \gg 1$), we gather evidence from in situ rheo-NMR measurements that the imposition of shear reduces the motional correlation time τ_c with increasing shear rate. We also find that the restoration of relaxation times, upon cessation of shear, is seen to occur over a much larger time scale (ca. 20 h). This has been interpreted by taking recourse to the postulate of the slow re-formation process in the framework of the energetically cross-linked transient network model (ECTN) proposed recently by our school.

Introduction

Studies of polymer solutions and melts under shear constitute the core of polymer rheology. Conventional rheological measurements such as viscosity, modulus, etc., relate to the changes that occur at a macroscopic level in a sheared sample, which in turn are linked to the changes occurring at a molecular level. However, the indirect inferences so drawn have to be supported by direct measurements of the changes that take place in molecular orientation and configuration in polymers under the influence of a shear field. These have been investigated by neutron scattering,[1] X-ray scattering,[2] and rheooptical techniques.[3] However, these methods are somewhat restrictive due to specific forms of the samples. For example, the requirement of very thin films in the case of flow birefringence and infrared dichroism poses an inherent limitation of using these techniques. Moreover, some surface phenomena also complicate the analysis of the results. In recent times, rheo-NMR has emerged as a potential tool to study the microscopic behavior of polymer solutions subjected to shear.[4]

In rheo-NMR, the polymeric fluid is sheared in a shearing device conforming to cone and plate or couette geometry, and the NMR signals are recorded. The first design of a cone and plate arrangement for the electromagnet-based NMR spectrometers was described by Nakatani et al.[4] This apparatus was found to offer advantages, since the angle between the direction of shear field and the main magnetic field B_0 could be varied within a restricted range of 30° to monitor and study the anisotropic manifestation of the shear field on ^{1}H NMR spectra. Further, they demonstrated the phenomenon of shear-induced phase transition in a LCST polymer, poly(vinyl methyl ether) [PVME], by using rheo-NMR. The adaptation of a cone and plate and a couette cell arrangements for the superconducting magnet was reported by Grabowski and Schmidt[5] and by Callaghan and Gil,[6] respectively. Rheo-NMR experiments between concentric cylinders employing an air-driven spinning arrangement to produce shear have been used in the past to study the Taylor vortex flows and couette shear flows.[7,8] Lukaschek et al.[9] reported deuterium NMR measurements on a hexagonal lyotropic liquid crystal using a NMR viscometer having cone and plate geometry with the cone axis parallel to the main magnetic field direction. Both these approaches demonstrate the manifestation of shear-induced orientation effects in the resulting NMR spectra. Whereas in proton NMR shear-induced changes affect the residual proton−proton dipolar interactions, the deuterium NMR, which requires ^{2}H isotopic labeling, exploits shear-induced changes in residual quadrupolar line shapes to be noticed in the observed ^{2}H NMR spectra. The spectral changes could be related to the degree of induced order due to shear.

An attractive alternative approach would be to monitor shear-induced changes in the nuclear spin relaxation, both in situ and upon cessation of the shear. The benefit of using proton spin relaxation is at once clear. The mechanism of proton relaxation for polymer solutions, such as poly(acrylamide) used in the present demonstration, is purely dipolar, and the shear-induced changes will be reflected in proton relaxation times. Further, in a molecule such as poly(acrylamide), relaxation times can be measured under high-resolution conditions, which offer unique opportunities to monitor and measure the changes in the relaxation times at specific sites and gather insights into the shear-induced changes that occur at the segmental level. We will show that such measurements can be potentially carried out with increased sensitivity under shear using a simple coaxial cylinder arrangement adaptable on a superconducting magnet.

In this paper, we describe a simple shearing device, which can be easily adapted on any commercial super-

* To whom correspondence should be addressed at: Director General, Council of Scientific and Industrial Research, Anusandhan Bhawan, 2 Rafi Marg, New Delhi- 110 001, India. Fax (91-11)3710618, e-mail dgcsir@csir.res.in.

10.1021/ma010938s CCC: $22.00
Published on Web 12/01/2001

conducting NMR spectrometer. No stepper motor driven shafts with suitable nonmagnetic gear assembly, such as used by previous workers,[4−6] need to be incorporated on a specially fabricated probehead. Our shearing device of couette geometry is rather easy to set up, and it facilitates quick NMR spectral and relaxation measurements in situ. Further, the relaxation times could be measured as a function of shear rate to monitor the microdynamic response of the polymer chains to the applied shear field. We have built such a device and used it for in situ rheo-NMR relaxation time measurements on dilute poly(acrylamide) solutions. The objective of the present work is twofold. First, we show that proton relaxation times can be easily and accurately measured under stagnant and in situ shearing conditions. Second, we show that the interpretation of the relaxation data obtained by us provides the first direct experimental evidence for the validity of the energetically cross-linked transient network (ECTN) model,[10] proposed from our school to explain the anomalous rheological behavior of PAM solutions.

PAM was chosen not only because of its industrial importance but also because it is the most popular choice as a model fluid in rheology.[11−14] Besides this, PAM solutions had shown peculiar rheological and flow behavior, such as double overshoots,[11] uncharacteristically long restoration times,[15] stress-induced phase separations,[16] etc. Lele and Mashelkar[10] recently developed the framework of an energetically cross-linked transient network (ECTN) model to explain these anomalies. We will demonstrate later that the in situ rheo-NMR measurements provide the molecular level insights to give credence to the ECTN model advocated by them. We now provide a brief background of the challenge posed by some of the unexplained anomalies, so that our focus on using the rheo-NMR for elucidating these will become clear.

ECTN Model and the Anomalous Rheological Behavior of PAM Solutions. Transient network theories are best suited to explain the dynamics of concentrated polymeric systems. Development of such theories started with Lodge's network model[17] and its subsequent modifications.[18] In these models, the network was considered to be formed through chain entanglements−disentanglements processes. Although these theories can predict various rheological phenomena, such as shear thinning, stress overshoots, stress relaxation, etc., they cannot predict the unusual behavior of the rheology of some of the polymers, as in the case of PAM. Consider, for instance, the long restoration times that are of the order of hours or days. The predicted time scales emanating from such theories will be related to the time scales over which the chain entanglements remain effective, namely, a few seconds, which are clearly the orders of magnitude smaller than the large restoration time scales.

It was observed by Kulicke et al.[11] that when a solution of PAM in ethylene glycol or formamide was sheared above a certain shear rate, the shear stress growth curve showed a double overshoot. A second overshoot of a very large magnitude was also observed in the first normal stress measurements, which was then followed by a fracture like stress decay indicating the breakage of a gel. Further, after reaching a steady-state stress, the second overshoot was not observed when the shear was restarted after cessation for 60 min. Both the presence of the second overshoot and the long time scales over which the solution remained unrelaxed were unusual and had remained unexplained.

Table 1. Restoration Times and Characteristic Molecular Relaxation Times for Polyacrylamide Solutions[a]

polymer solution concn (%)	restoration time (range in min)	relaxation time (ms)
4.6×10^{-3}	4−5	60.0
5.5×10^{-3}	5−6	80.0
6.6×10^{-3}	7−8	120.0
7.8×10^{-3}	9−10	200.0
1.0×10^{-2}	14−15	340.0

[a] These values were calculated from the terminal settling velocities of spheres in a ball dropping experiment.[22]

Bissgaard,[19] Cho et al.,[20] and Ambeskar and Mashelkar[21] conducted experiments wherein they dropped spheres in aqueous PAM solutions. They measured the terminal settling velocities of these spheres and showed that the settling velocities of identical spheres, dropped consecutively along the same path in a PAM solution, kept increasing until a saturation velocity was reached. In a low molecular weight liquid, such as water, if a sphere is dropped, its original structure, which is disturbed by the shearing of the sphere, is restored instantaneously (say 10^{-12} s). In a dilute polymer solution, where no energetic interactions exist (such as polystyrene in toluene), again the structure is restored in time scales, which are of the order of molecular relaxation times (say 10^{-2}−1 s). Therefore, in such liquids, if two consecutive balls are dropped within a span of, say 5 s, one gets the same terminal settling velocity. But this was not the case in poly(acrylamide) solutions. It turned out that, although the molecular relaxation times were of the order of 50−350 ms, the times taken for restoring the same structure (as measured by the time taken to reach the same terminal velocity, referred to as restoration times) were of the order of several minutes or hours. For PAM solutions, which are more dilute (viz. 0.005−0.01%) than the ones used in our work, the data obtained by Ambeskar[22] are shown in Table 1. Lele and Mashelkar[10] argued that they have a common physical basis, which originates from the ability of PAM solutions to form energetic transient networks. In PAM, the energetic cross-links of the polymer network are formed by hydrogen bonding between polar groups on the polymeric chains. The probability of forming interchain hydrogen bonds increases with an increase in the polymer−solvent interaction parameter. A schematic view of the formation and breakage of hydrogen bonds in PAM is shown in Figure 1.

The energy of hydrogen-bonding interaction is of the order of kT, where k is Boltzmann's constant and T is the absolute temperature, and it is an order of magnitude smaller than that of a C−C covalent bond. Therefore, the energetic interactions due to hydrogen bonding can be broken more easily than the covalent bonds. Strong shear and extensional flows would have sufficient energy to easily break both intra- and interchain hydrogen bonds. The re-formation of the broken hydrogen bonds however requires that the polar groups of PAM come within the interacting distance (2−5 Å). The stretching of the individual coils caused by a shear field or elongational flow can aid in the formation of interchain hydrogen bonding to cause an association of the molecular chains. The chain orientations/disentanglements can assist in building up of the hydrogen bonds by keeping the chains in a stretched state. The probability of successful bonding in fact would depend on

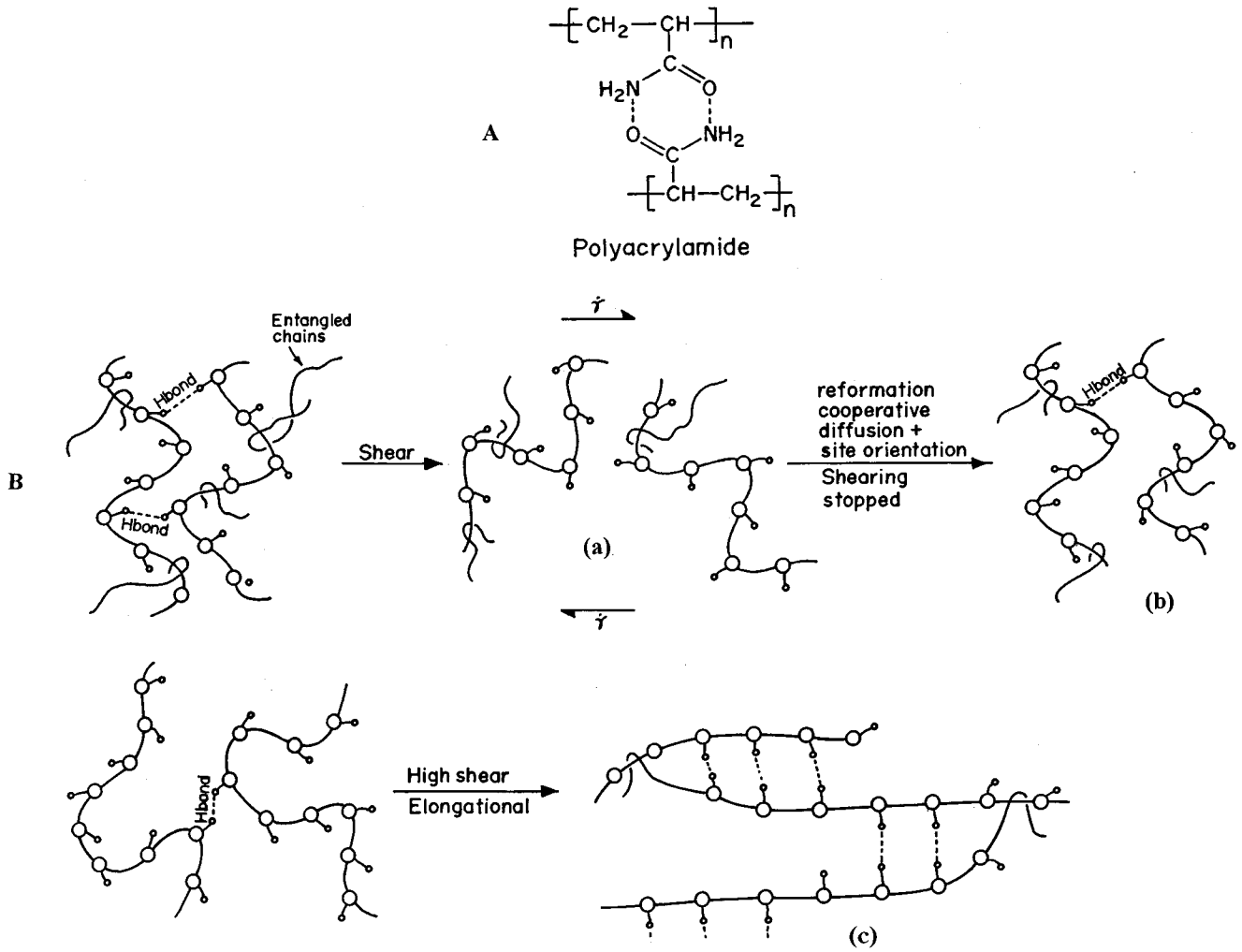

Figure 1. (A) Interchain hydrogen bonding in poly(acrylamide) and (B) a schematic molecular picture of (a) breakage of hydrogen bonds by shear, (b) re-formation on stopping shear, and (c) formation of ladderlike structures at high shear or high elongation rates.

the proper orientation of the approaching donor−acceptor groups. When driven by thermodynamic (free energy) forces, the restoration process would involve cooperative mobility of the network, which inherently has slow dynamics. Further, it is envisioned that staggered ladderlike structures would form by a zipping-like effect at high shear or elongation rates, wherein the polar groups located next to an already formed hydrogen bond find it relatively easier (in an entropy sense) to form a bond. In essence, cooperative effects are crucial in the formation of hydrogen-bonded structures in the case of PAM solutions, and the large restoration times that have been noticed are implicit from such considerations. The re-formation process is shown schematically in Figure 1B. Lele and Mashelkar[10] could explain the anomalous results obtained by Kulicke et al.[11] on double overshoots by using the ECTN model. They also provided a qualitative explanation for the long restoration times in the falling sphere experiments. However, no molecular level evidence was provided by them to support the ECTN model.

Our rheo-NMR studies based on spin−lattice and spin−spin relaxation times should be able to provide a direct evidence for the breakage as well as the slow re-formation process depicted in Figure 1. This stems from the fact that the relaxation times are sensitive to the polymer mobility and the correlation time involved. Since we can use rheo-NMR to probe the motional dynamics of the polymeric system at the segmental level, we believe that we can provide the first experimental evidence for the validation of the key assumptions in the ECTN model.

Experimental Section

Couette Cell for Rheo-NMR on a Superconducting NMR Spectrometer. The in situ rheo-NMR device of couette cylinder geometry built by us is shown in Figure 2. This apparatus was designed to work with an existing Bruker MSL-300 FT-NMR spectrometer, operating at a proton frequency of 300.13 MHz, and a diffusion-microimaging or a standard liquids probehead which takes 10 mm (o.d) sample tubes. The polymer solution was held in the 10 mm sample tube, and its position was preadjusted to maintain the sample in the homogeneous B_0 field. This formed the outer cylinder of the couette cell. To shear the sample, a glass spindle of diameter 8 mm was attached to a 5 mm air turbine, and its height was carefully adjusted by using a sample positioning gauge. The air turbine was pneumatically lowered into the magnet, and when it was positioned inside the magnet bore, the entire setup formed a coaxial cylindrical geometry with a gap size of 0.5 mm between the rotating inner and stationary outer cylinder (see Figure 2). The outer surface of the spindle was ground to impart roughness to the surface for an effective shearing. The high-resolution sample spinning arrangement, the pneumatically regulated drive air supply, and the optically sensed rotational speed measurement on the MSL-300 console allowed us to employ spinning speeds of 2−50 Hz, which could be precisely controlled and measured to within 1 Hz using dry

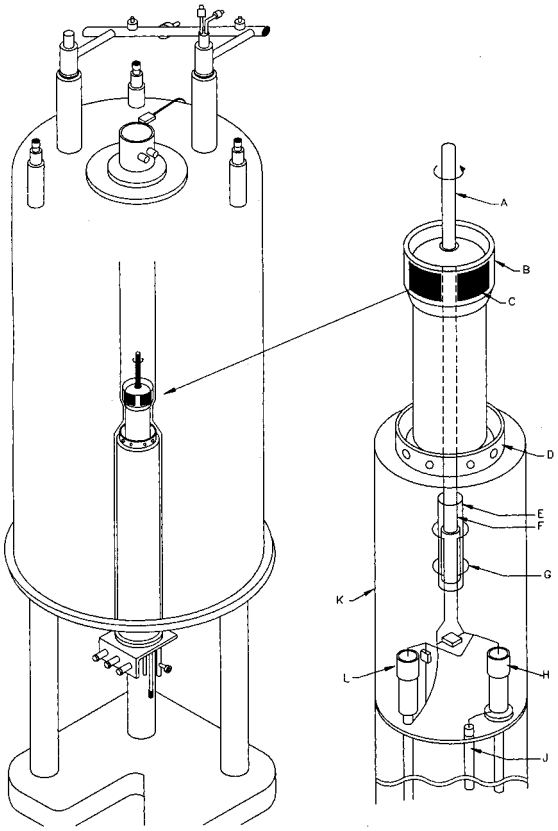

Figure 2. Schematic of the couette cell arrangement using high-resolution sample spinning facility provided on any high field supercon FT-NMR spectrometer. The seating of the couette within the room temperature bore of the supercon magnet is seen on the left. Expanded view of the couette cell is shown on the right. The various labels correspond to (A) the glass spindle (5 mm o.d) extending from the inner cylinder, (B) the nylon 5 mm rotor, (C) marks for optical sensing of rotor speed, (D) holes for the spinning air, (E) outer cylinder (10 mm o.d., standard NMR tube), (F) inner cylinder (8 mm o.d.), (G) saddle rf coil, (H) tune capacitor, (L) match capacitor, and (K) probe body.

air. For an annular gap of 0.5 mm, used in the present arrangement, this corresponded to shear rates ($\dot{\gamma}$) of 18−450 s^{-1}.

In Situ Relaxation Time Measurements. The relaxation time measurements were performed by using the $\pi-\tau-\pi/2-$Acq inversion−recovery[23] (T_1) and $\pi/2-(\tau-\pi-\tau)_n-$Acq Carr−Purcel−Meiboom−Gill[24] (T_2) pulse sequences, with a short τ delay for the T_2 sequence. Here n corresponds to the number of times the π pulse is applied, and the total time ($2n\tau$) is systematically incremented by increasing n in the pulse sequence. By the CPMG method, we could thus eliminate the diffusional contribution to the decay of spin echo intensity, thus ensuring a true T_2 decay for the proton magnetization. Prior to the relaxation measurements, the poly(acrylamide) solution was placed in 10 mm tube, and the length of the tube was adjusted to position the sample in the center of the rf coil. The experiments were performed by deactivating the field sweep and setting the main B_0 field to the desired value. The homogeneity of the magnetic field over the sample volume was improved by adjusting the room temperature shims on the FID prior to the experiment. The $\pi/2$ pulse used was 27 μs, and 8−16 transients were accumulated with a recycle delay of 5 s. The τ delay in the CPMG pulse train was chosen to be 1 ms to minimize the diffusion contribution to the spin-echo intensity decay. Prior to Fourier transformation, the time domain signal was multiplied by an exponential decay function with a line width of 5 Hz. The T_1 and T_2 data were analyzed using an on-line Bruker utility program SIMFIT. The ^{1}H−^{1}H 2-D NOESY experiment was performed on a Bruker DRX-500

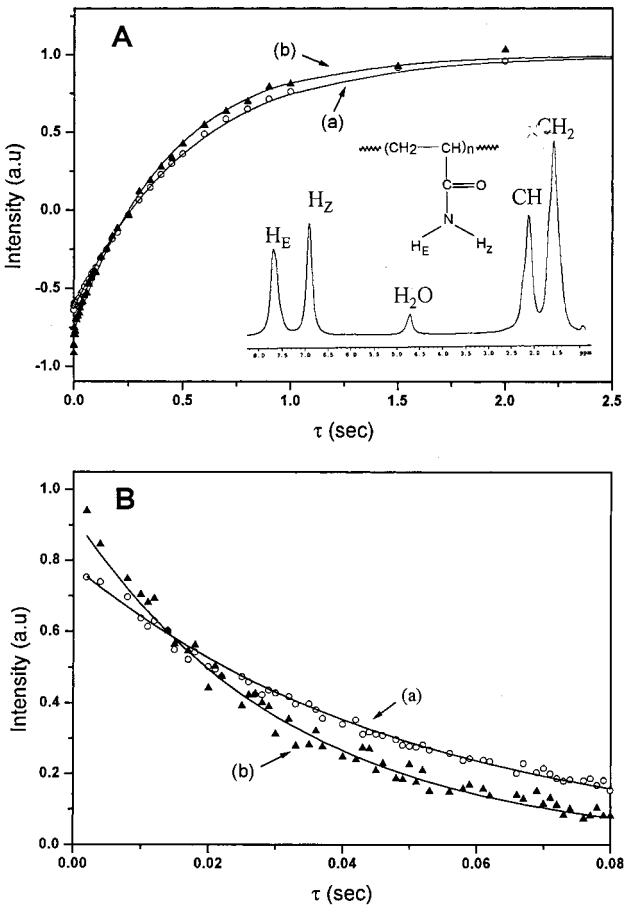

Figure 3. (A) Inversion recovery T_1 data of CH proton and "best-fit" curves calculated by least-squares analysis (solid line) for unsheared (○) and sheared ($\dot{\gamma}$ = 45 s^{-1}) (△) 2% poly-(acrylamide) solution in water. The corresponding CP-MG T_2 data and analysis are shown in (B). Inset shows the ^{1}H spectrum of PAM in H_2O. The intense water signal is suppressed using a WATERGATE pulse sequence. The signal assignments are also shown.

NMR spectrometer by using a 5 mm inverse probe equipped with a *z*-gradient. To suppress the strong water signal, a WATERGATE[25] pulse sequence was employed, and a mixing time of 750 ms was found to be optimal for revealing the various cross-peaks. Other relevant parameters are given in the figure caption.

PAM used in the present study was a commercial sample obtained from Dow Chemicals. The molecular weight was 5.6 × 10^5 and M_w/M_n = 1.76. Samples for in situ rheo-NMR measurements were prepared in H_2O and D_2O (99.9%) separately in the concentration of 1 and 2% (wt/wt) and homogenized for 5 days at room temperature before undertaking the measurements.

Results and Discussion

Proton Spin−Lattice and Spin−Spin Relaxation in PAM. For PAM in H_2O, the proton signals belonging to the main chain (CH, CH_2) and the side chain ($NH_2 \rightleftharpoons H_E$, H_Z) are clearly resolved as shown in Figure 3A (inset). The intense water signal in the spectrum is suppressed using the WATERGATE pulse sequence. This facilitates the determination of relaxation times of the main chain and side chain protons. Despite the intense water signal, the polymer signals could be detected with sufficient intensity to enable relaxation time measurements to be made in H_2O solutions. The dynamic range problem was however overcome in the D_2O solutions where the polymer protons could be

Table 2. Proton Spin−Lattice and Spin−Spin Relaxation Data for 1.0% PAM Solution in D_2O

	T_1 (ms)		T_2 (ms)	
conditions	CH	CH_2	CH	CH_2
stagnant ($\dot{\gamma} = 0$)	576	290	62.1	24.5
in situ (shearing at $\dot{\gamma} = 17\ s^{-1}$)	536	285	47.0	22.0
in situ (shearing at $\dot{\gamma} = 127\ s^{-1}$)	500	266	22.0	21.0
in situ (shearing at $\dot{\gamma} = 255\ s^{-1}$)	451	246	29.6	19.9

Table 3. Proton Spin−Lattice and Spin−Spin Relaxation Data 2.0% PAM Solution in D_2O

	T_1 (ms)		T_2 (ms)	
conditions	CH	CH_2	CH	CH_2
stagnant ($\dot{\gamma} = 0$)	534	293	50.7	25.6
in situ (shering at $\dot{\gamma} = 42\ s^{-1}$)	458	269	41.2	24.0
in situ (shearing at $\dot{\gamma} = 85\ s^{-1}$)	412	263	31.8	21.8
immediately after stopping shear	473	276	47.3	26.0
14 h after stopping shear	505	277	45.0	24.0
22 h after stopping shear	538	288	37.0	23.0

Table 4. Proton Spin−Lattice and Spin−Spin Relaxation Data for 2.0% PAM Solution in H_2O

	T_1 (ms)			
conditions	NH_E	NH_Z	CH	CH_2
stagnant ($\dot{\gamma} = 0$)	235	259	390	278
in situ (shearing at $\dot{\gamma} = 42\ s^{-1}$)	200.8	235.5	330.0	259
immediately after stopping shear	222.0	253.9	388	255

detected with increased intensity. The amide protons remained undetected in the proton spectra of PAM in D_2O solution due to the deuterium exchange of amide protons. Measurements in H_2O and D_2O solutions may additionally give clues about the importance of dipolar relaxation pathway between the water protons and the polymer protons.[26] In our well-shimmed magnet, no noticeable changes in proton line width or line shape could be observed, irrespective of whether the sample is sheared or not. The line width of the polymer peaks was typically 70 Hz. On the basis of the T_1 and T_2 values we have measured, we calculate the lifetime broadening due to T_1 to be <1 Hz and due to T_2 to be <15 Hz. This shows that the observed line widths are not limited by T_1 or T_2 relaxation and that they are attributable to chemical shift dispersion effects in this high molecular weight polymer and/or to the residual inhomogeneity introduced by the couette cell.

We show in Figure 3 representative experimental spin−lattice (A) and spin−spin (B) relaxation time measurements carried out on PAM solution in the absence and presence of shear. In each case, the relaxation data were collected before shearing ($\dot{\gamma} = 0$), during shearing ($\dot{\gamma} = 45, 85\ s^{-1}$), and after stopping the shear and up to 22 h. Typically, about 30 min was required to conduct a T_1 or a T_2 experiment. This time is however much shorter than the restoration times that tend to bring the polymer system back to the equilibrium configuration, so that the measurement carried out at a certain time after the cessation of shear has minimal time averaging effects. In all cases the T_1 and T_2 decays were found to be exponential (see Figure 3), so that the T_1 and T_2 relaxation data could be fitted to the equations $M(\tau) = M_0[1 - 2\exp(-\tau/T_1)]$ and $M(\tau) = M_0 \exp(-\tau/T_2)$, respectively, in each case. The SIMFIT results of the relaxation data analysis at each shear rate for 1 and 2% PAM solutions are summarized in Tables 2−4.

Inspection of T_1 and T_2 data presented in Tables 2−4 for each of H_2O and D_2O runs at once show that the proton spin relaxation has a strong dependence on the shear field. We observe that the onset of shear tends to enhance the relaxation rate of the unsheared polymer both for the longitudinal and transverse relaxation. We also observe that increase in relaxation rates ensue with increasing shear rates. Noting that the largest change occurs in T_1 relaxation during shear, we inspected the T_1 value upon cessation of shear. We find that this value is higher than the value measured during shear at the largest shearing rate. However, the recovery of T_1 value toward that of the static unsheared sample was unusually slow. The complete restoration of longitudinal relaxation time takes about 22 h. The T_1 results thus provide the time scale over which the stress relaxation takes place to bring the polymeric system into an equilibrium conformation. We will later provide a molecular level insight for the occurrence of such a long time scale for restoration.

The spin−lattice relaxation rates are determined entirely by the dipolar relaxation mechanism, and further, the same mechanism holds good at all the shear rates. The decreasing relaxation times at increasing shear rates clearly point to a microdynamic response of the polymer chains to the imposition of shear. Similar parallel observations are noticed in T_2 relaxation as well. More importantly, we observe that the T_2 values are typically an order of magnitude smaller than T_1 values. However, we find that our T_2 values are longer than those reported by Callaghan and Gil,[6] who have recently studied shear-dependent T_2 measurements in PAM solutions. Independent T_2 measurements using a Hahn spin-echo sequence indeed show reduced T_2's as Callaghan and Gil have observed. Such a reduction in T_2 can arise from the diffusional effects, and it is not clear whether this was taken into consideration in the previous T_2 study.[6] Further, we find that the PAM used by them is a 60:40 copolymer of acrylamide and sodium salt of acrylic acid, whereas our system is a partially hydrolyzed (~10%) PAM. Moreover, the molecular weight of the PAM used by them is greater than 10^7, whereas ours is 5.6×10^5. Certainly, these can play a role in determining the exact T_2 values, although as we have commented, the diffusional effects have to be eliminated in the T_2 measurements.

Dipolar Relaxation in PAM and the Motional Regime. In PAM, modulation of dipolar interactions for the backbone protons (CH, CH_2) by polymer mobility is the dominant mechanism for their proton spin relaxation. The dipolar interaction for the observed resonances emanates from proton−proton couplings within the same group, as for CH_2 and NH_2, or with the proton(s) in the immediate vicinity, as for CH. To derive motional information from T_1, one must first ascertain the motional regime in which the proton relaxation occurs. This is because the same value of T_1 is obtained for two different correlation times, one that is shorter than the Larmor period (ω_0^{-1}) and the other longer, when T_1 relaxation occurs away from the $T_{1\ min}$.

To identify the motional regime in which the proton spin relaxation of an unsheared PAM occurs, we have resorted to carrying out phase-sensitive 2-D $^1H-^1H$ NOESY experiments on 2% poly(acrylamide) in 90% H_2O and 10% D_2O mixture. The rationale for doing this experiment is as follows. Motional modulation of intramolecular dipolar interactions in PAM would provide efficient cross-relaxation pathways and promote the development of nuclear Overhauser enhancements (nOe).

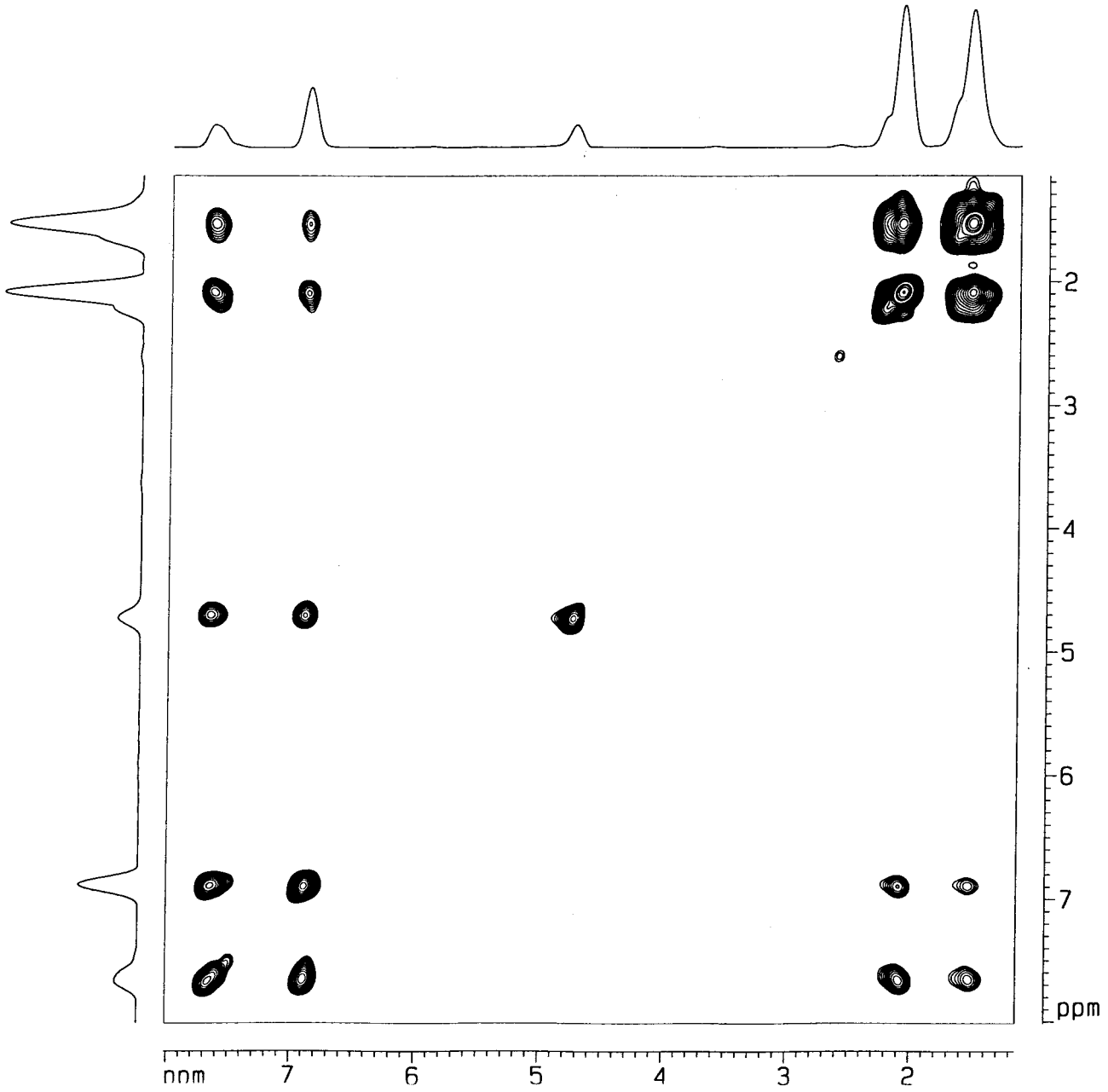

Figure 4. The 500.13 MHz water suppressed 2-D ^{1}H−^{1}H phase-sensitive NOESY contour plot showing the diagonal and cross-peaks in unsheared 2.0% poly(acrylamide) solution in H_2O. All the cross-peaks occur with a positive sign. $\tau_m = 750$ ms.

For a polymeric system whose motions are characterized by the reorientational correlation time τ_c, the steady-state nOe is given by[27,28]

$$\eta_{nOe}^{max} = \sigma_{HH}/\rho_{HH} \quad (1)$$

where σ_{HH} and ρ_H denote the cross- and autorelaxation rates, respectively. Equation 1 implies that the saturation of one of the protons increases or decreases the signal intensity of the other dipolar coupled proton(s) from the equilibrium value, depending on whether nOe is positive or negative. For the homonuclear case, as we have for the protons of PAM, the sign of nOe is embedded in the cross-relaxation rate σ_{HH}, which is given by

$$\sigma_{HH} = W_2 - W_0 \quad (2)$$

where W_2 and W_0 are the double and zero quantum transition probabilities, respectively, whose magnitudes are determined by the Larmor frequency (ω_0), the correlation time for the motion (τ_c), and the internuclear distances, r. Since the relative importance of W_2 over W_0 determines the sign of nOe, an experimental determination of the sign of nOe would provide clues about the motional regime in which the cross-relaxation occurs. Specifically, steady-state nOe is positive in the short correlation regime ($\omega_0\tau_c \ll 1$) and is negative and twice as large in the long correlation regime ($\omega_0\tau_c \gg 1$). In the 2-D ^{1}H−^{1}H NOESY experiment, when the cross-peaks develop due to the operation of nOe, their absolute sign can be determined from experiments performed in the phase-sensitive mode.[29]

We show in Figure 4 the 2-D ^{1}H−^{1}H NOESY contour plot for a 2% PAM in 90% H_2O and 10% D_2O. The intense water signal has been very effectively suppressed by the WATERGATE[25] solvent suppression scheme to show a clear depiction of polymer−polymer

cross-peaks. Further, by conducting experiments in 90% water, the NH_2 protons remain protonated, and the cross-peaks within the NH_2 group and between NH_2 and CH, CH_2 groups can also be revealed in the 2-D experiment. It is important to note that the amide proton cross-peaks can develop due to cross-relaxation and/or chemical exchange. However, it was shown in our earlier work[26] that for the amide protons cross-relaxation dominates over chemical exchange at ambient temperature. We observe that the cross-peaks between various polymer protons within the repeat unit are intense, and further, they occur with positive absorption (same as the diagonal), providing evidence that the nOe is negative in sign. Temperature-dependent T_1 measurements of unsheared poly(acrylamide) solution also show a reduction in T_1 values upon increase in temperature. Thus, we verify from our 2-D NOESY experiment that the motional dynamics of unsheared PAM occurs in the long correlation regime ($\omega_0\tau_c \gg 1$) at ambient temperature.

Having verified that the proton relaxation occurs in the long correlation regime ($\omega_0\tau_c \gg 1$), we now explain the observed decrease in proton T_1 upon increasing shear rate using the BPP theory.[30] The relevant BPP equation for the relaxation operating through the dipolar mechanism is

$$(1/T_1)_i = C_i[J^{(1)}(\omega_0) + J^{(2)}(2\omega_0)] \qquad (3)$$

where C_i is the strength of the dipolar interaction which is modulated by polymer mobility and is given by $C_i = \sum\gamma^4\hbar^2/r_{ij}^6$, where the subscript i denotes the ith proton whose relaxation is observed and j denotes the various protons which are dipolar coupled to the ith proton. It may be noticed that the overall strength of the dipolar interaction, which governs the observed relaxation, is represented by the summation in C to include contributions from directly bonded and nonbonded protons within a certain distance (3 Å). In eq 3, $J(\omega_i)$ denotes the spectral density function given by

$$J(\omega_i) = \tau_c/(1 + \omega_i^2\tau_c^2) \qquad (4)$$

where the molecular mobility of the polymeric system is defined by the reorientational correlation time τ_c. Equation 3 governs the observed T_1 through the dynamics of the system contained in eq 4. We envisage that in our isotropic poly(acrylamide) solution there are no orientational effects due to shear insofar as dipolar interactions within the repeat unit are concerned, and the observed changes in T_1 must therefore necessarily arise from changes in τ_c. Considering that 2-D NOESY experiments in unsheared 2% PAM solution has shown that molecular mobility occurs in the long correlation regime ($\omega_0\tau_c \gg 1$), the observed decrease in T_1 upon shear undoubtedly points to a decrease in τ_c due to shear. The decrease in motional correlation time τ_c for the polymer, when subjected to a shear field, must arise from the decreased motional constraints for the polymer segments. As mentioned earlier, PAM exhibits a transient network behavior due to the hydrogen-bonding interactions and entanglements.[11] The shear field is capable of breaking some of these hydrogen bonds (see previous section), which in turn removes motional constraints imposed by hydrogen bonding and entanglements. This would result in large reduction in the motional correlation time τ_c, hence enhancing the measured proton spin−lattice relaxation rates in the slow motion regime. While the decrease in T_1 with increasing shear rates corroborates our hypothesis (slow motion regime and increase in mobility), T_2 is, however, marginally affected with a slight tendency to decrease. Since T_2 senses mobility near zero frequency (apart from the motion at high frequency), the low-frequency component due to shear-induced anisotropy could probably account for the observed trend in T_2. On the whole, our in situ relaxation time measurements provide molecular level insights on the response of the polymeric system to shear.

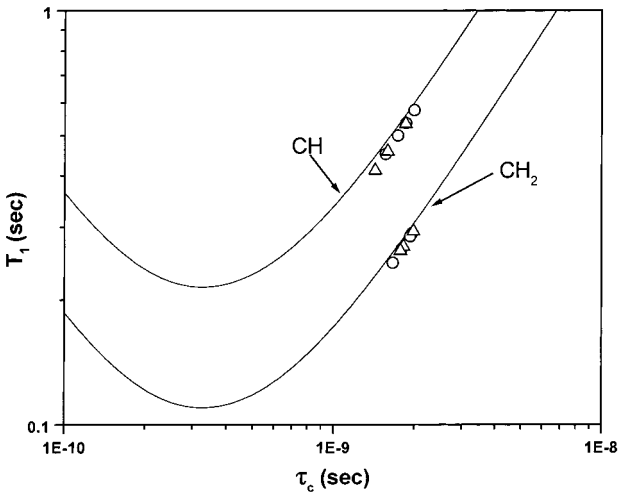

Figure 5. Plot of proton T_1 as a function of the motional correlation time τ_c using eq 3 (see text). The T_1 curve was generated using $C = [\gamma^4\hbar^2/r^6]$ to be 1.201×10^{10} and 0.614×10^{10} s^{-2} for CH_2 and CH protons, respectively. The correspondence between the shear-dependent reduction in T_1 values and the reduction in T_1 with increasing mobility in the long correlation regime is shown. The experimental data points correspond to (○) 1% and (△) 2% PAM solution in D_2O.

We show in Figure 5 the correspondence between the increasing enhancement in the spin−lattice relaxation rate with increasing shear rate and the enhanced relaxation rate due to enahnced molecular mobility occurring in the long correlation regime. Theoretical BPP curves were calculated using eqs 3 and 4, and C is 1.201×10^{10} and 0.615×10^{10} s^{-2} for the CH_2 and CH protons, respectively,[31] to cover 2 orders of magnitude in the motional correlation time, i.e., from 10^{-10} to 10^{-8} s. Having identified that the motional regime is in the long correlation limit ($\omega_0\tau_c \gg 1$), the room temperature T_1 value for the unsheared PAM allows us to deduce τ_c to be 0.96×10^{-9} s from eqs 3 and 4 using the above values for the dipolar relaxation constant C. We show in Figure 5 the correspondence between the experimental T_1 data and the reduction in T_1 as a function of τ_c as calculated by the BPP curves for the CH_2 and CH protons. Here the experimental values of T_1 obtained at different shear rates have been used to estimate τ_c at each shear rate using eqs 3 and 4, under the condition $\omega_0\tau_c \gg 1$, together with the above values for C for CH and CH_2. We observe that the experimental data points satisfactorily fall on the theoretical BPP curve and show that a reduction in τ_c upon increasing shear rate indeed occurs. For the maximum shear rate that we have employed ($\dot{\gamma} = 255$ s^{-1}), the reduction in τ_c from the unsheared state, as inferred from Figure 5, amounts to ~120 ps.

Interpretation of NMR Relaxation Data Based on ECTN Model. In the following we provide molecular

level insights into the shear-dependent proton spin relaxation we have observed based on the above framework. We first consider the influence of shear in the in situ measurements. Based on the above ECTN model where energetic cross-links in PAM are attributed to hydrogen bonding, a recourse to Figure 1A shows that the amide NH of one chain (donor) is hydrogen bonded to the amide carbonyl of the other chain (acceptor) and vice versa. These hydrogen-bonding sites are the ones more susceptible to breakage by shear. When this occurs, one ought to expect a large change in the relaxation times for the protons in the immediate neighborhood of the hydrogen-bonding sites, namely, the amide protons themselves (involved directly in hydrogen bonding) and the backbone CH protons of the main chain which show a strong dipolar interaction with the amide protons. This latter feature is also evident from the 2-D NOESY data of Figure 4 where the amide to CH cross-peak intensity is found to be stronger than the amide to CH_2 cross-peak. Further, considering that the breakage of hydrogen bond merely serves to decrease the motional correlation time and not change the geometry, we expect a lager reduction in T_1 and T_2 to be noticed for the amide protons and the CH proton of the main chain, compared to that of CH_2. For the amide protons H_E and H_Z, which are involved in hydrogen bonding, we find that the T_1 of H_E is shorter than that of H_Z both under stagnant and sheared conditions. On the basis of the 2-D NOESY data (see Figure 4) and in accordance with our earlier study[26] of PAM, we observe that the H_E to CH cross-peak develops with a stronger intensity compared to the corresponding one between H_Z and CH. Stereochemically H_E is proximal to CH, causing the stronger development of the cross-peak with CH. For H_Z, however, cross-relaxation occurs through H_E since the direct H_Z to CH cross-relaxation pathway is attenuated by a longer distance. This is also reflected in T_1 measurements where we observe a larger relaxation rate for H_E over H_Z at all shear rates. Since the CH proton of the main chain shows a strong dipolar interaction with the amide protons, we ought to expect a larger change in T_1, upon shear, for the CH proton than the CH_2 protons. This is indeed observed in our in situ relaxation measurements where we observe that while the relaxation times for all the proton environments are affected by shear, the largest change is observed for the CH proton, in both T_1 and T_2 (in 1%, 2% D_2O, and 2% H_2O) as well as for H_E and H_Z of NH_2 (in 2% H_2O) (see Table 4), over the changes noticed for CH_2 proton relaxation times.

Restoration of T_1 and T_2 upon Cessation of Shear. A salient feature of our proton relaxation time measurements is that the restoration of T_1 or T_2 values, upon the cessation of the shear, toward the original unsheared condition takes several hours (ca. 20 h), which is considerably longer than the molecular relaxation times which are of the order of hundreds of milliseconds. The slow recovery of T_1 and T_2 values to those observed for the unsheared polymer solution is in accord with the ECTN model, where it is emphasized that slow cooperative motions assist the process of reformation of hydrogen-bonded networks to cause the slow restoration of the polymer networks. An inspection of the final T_2 values measured after 22 h from the cessation of shear reveals that the relaxation times are not fully restored to the original values. This indicates that the original equilibrium configuration of the polymer is not necessarily retained in the fully relaxed network following the restoration process on the time scales at which studies were undertaken by us. Furthermore, the restoration times observed by us are more than those reported by Callaghan and Gil.[6] This could be attributed to the fact that the extent of hydrolysis in our system (∼10%) is different from that of their system. The transient networks in PAM are formed by physical entanglements as well as by energetic interactions formed by H-bonding. On stopping shearing, the breakage of physical entanglements is restored relatively quickly, but those due to energetic interactions take longer time due to slow cooperative diffusion, orientation, etc. Recovery times for system with higher levels of H-bonding will, therefore, be longer. Our solutions are partially hydrolyzed, and therefore the recovery times in our case are longer.

Conclusions

We have shown that a simple but elegant method of doing in situ rheo-NMR experiments can be easily implemented on modern NMR spectrometers. In situ proton spin−lattice and spin−spin relaxation time measurements have been carried out using a couette cell geometry on poly(acrylamide) solutions. A shear rate-dependent decrease in both longitudinal and transverse relaxation times is noted. Breakage of energetic cross-links (hydrogen bonding) due to shear is shown to cause a decrease in the motional correlation time in the long correlation regime, causing an increase in the relaxation rates. The restoration of T_1 and T_2 to the equilibrium unsheared value, upon cessation of shear, depicts the recovery of the polymer system from the sheared state to the native equilibrium state via stress relaxation. We have found that this occurs over a much longer time scale of the order of several hours (ca. 20 h). The long restoration times are postulated to arise from the slow cooperative motions of the polymer chains during the re-formation of the energetic interactions. The dynamic rheo-NMR experiments thus provide the first molecular level evidence to the phenomenological ECTN model proposed by Lele and Mashelkar[10] to explain the anomalous rheological behavior of PAM solution.

References and Notes

(1) Dadmun, M. D.; Han, C. C. *Macromolecules* **1994**, *27*, 7522.
(2) Safinya, C. R.; Sirota, E. B.; Bruinsma, R. F. *J. Phys.: Condens. Matter* **1990**, *2*, SA365.
(3) Sondergaard, K.; Lyngaae-Jorgensen, J. *Rheo-physics of Multiphase Polymer Systems: Characterization by Rheo-optical Techniques;* Technomic Publishing Co. Inc.: Lancaster, Basel, 1995.
(4) Nakatani, A. I.; Poliks, M. D.; Samulski, E. T. *Macromolecules* **1990**, *23*, 2686.
(5) Grabowski, D. A.; Schmidt, C. *Macromolecules* **1994**, *27*, 2632.
(6) Callaghan, P. T.; Gil, A. M. *Macromolecules* **2000**, *33*, 4116.
(7) Vera, M.; Grutzner, J. B. *J. Am. Chem. Soc.* **1986**, *108*, 1304.
(8) Lacelle, S.; Cau, F.; Tremblay, L. *J. Phys. Chem.* **1991**, *95*, 7071.
(9) Lukaschek, M.; Grabowski, D. A.; Schmidt, C. *Langmuir* **1995**, *11*, 3590.
(10) Lele, A. K.; Mashelkar, R. A. *J. Non-Newtonian Fluid Mech.* **1998**, *75*, 99.
(11) Kulicke, W. M.; Kniewske, R.; Klien, J. *Prog. Polym. Sci.* **1982**, *8*, 373.
(12) Barnes, H. A.; Hutton, J. H.; Walters, K. *An Introduction to Rheology*; Elsevier Science: Amsterdam, 1989.
(13) Walters, K.; Tanner, R. I. The motion of a sphere through an elastic liquid. In *Transport Processes in Bubbles, Drops and Particles;* Chhabra, R. P., DeKee, D., Eds.; Hemisphere: New York, 1992.

(14) Agarwal, U. S.; Dutta, A.; Mashelkar, R. A. *Chem. Eng. Sci.* **1994**, *49*, 1693.
(15) Gheissary, G.; van den Brule, B. H. A. A. *J. Non-Newtonian Fluid Mech.* **1996**, *67*, 1.
(16) Fergusson, J.; Hudsen, N. E.; Warren, B. C. H.; Tomalarian, A. *Nature* **1987**, *325*, 234.
(17) Lodge, A. S. *Trans. Faraday Soc.* **1956**, *52*, 120.
(18) Bird, R. B.; Curtiss, C. F.; Armstrong, R. C.; Hassagar, O. Kinetic Theory. In *Dynamics of Polymeric Liquids*; Wiley: New York, 1987; Vol. 2, Chapter 20, p 353.
(19) Bisgaard, C. *J. Non-Newtonian Fluid Mech.* **1983**, *12*, 283.
(20) Cho, Y. I.; Hartnett, J. P.; Lee, W. Y. *J. Non-Newtonian Fluid Mech.* **1984**, *15*, 61.
(21) Ambeskar, V. D.; Mashelkar, R. A. *Rheol. Acta* **1990**, *29*, 182.
(22) Ambeskar, V. D. Ph.D. Thesis, University of Bombay 1990.
(23) Slichter, C. P. *Principles of Magnetic Resonance*; Springer-Verlag: Berlin, 1990.
(24) Carr, H. Y.; Purcell, E. M. *Phys. Rev.* **1954**, *94*, 630. See also: Meiboom, S.; Gill, D. *Rev. Sci. Instrum.* **1958**, *29*, 6881.
(25) Piotto, M.; Saudek, V.; Sklenar, V. *J. Biomol. NMR.* **1992**, *2*, 661.
(26) Rajamohanan, P. R.; Ganapathy, S.; Ray, S. S.; Badiger, M. V.; Mashelkar, R. A. *Macromolecules* **1995**, *28*, 2533.
(27) Solomon, I. *Phys. Rev.* **1955**, *99*, 559.
(28) Neuhaus, D.; Williamson, M. *The Nuclear Overhauser Effect in Structural and Conformational Analysis*; VCH Publishers: Weinheim, 1989.
(29) In the 2-D NOESY experiment, positive cross-peak results due to chemical exchange or cross-relaxation occurring in the long correlation limit ($\omega_0\tau_c \gg 1$). The sign of the cross-peak is determined in the phase-sensitive NOESY experiment. However, the cross-realxation is distinguished from chemical exchange by conducting 2-D Overhauser experiments in the rotating frame (ROESY). Negative ROESY cross-peaks for poly(acrylamide) reveal the importance of dipolar cross-relaxation for amide protons (see ref 26).
(30) Abragam, A. *The Principles of Nuclear Magnetism*; Clarendon: Oxford, 1961.
(31) The dipolar relaxation constants $C_i = \sum[\gamma^4\hbar^2/r_{ij}^6]$ were calculated for the CH and CH_2 protons using a standard geometry for the bond lengths (C−H = 1.1 Å and tetrahedral bond angle of 109.5°) and considering proton−proton distances up to 3 Å for the various intramolecular interactions within the repeat unit of poly(acrylamide).

MA010938S